Talanta 80 (2010) 1452–1460

Contents lists available at ScienceDirect

Talanta

journal homepage: www.elsevier.com/locate/talanta

Sorption of As(V) from waters using chitosan and chitosan-immobilized sodium silicate prior to atomic spectrometric determination

Ezel Boyacı[a], Ahmet E. Eroğlu[a,*], Talal Shahwan[a,b]

[a] Department of Chemistry, İzmir Institute of Technology, Gulbahce, Urla 35430, İzmir, Turkey
[b] Department of Chemistry, Birzeit University, Ramallah, West Bank, Palestine

ARTICLE INFO

Article history:
Received 30 April 2009
Received in revised form
14 September 2009
Accepted 25 September 2009
Available online 3 October 2009

Keywords:
As(V)
As(III)
Sorption
Chitosan
Chitosan-immobilized sodium silicate

ABSTRACT

A natural biosorbent containing amine functional groups, chitosan, and a novel sorbent, chitosan-immobilized sodium silicate, were prepared and utilized for the selective sorption of As(V) from waters prior to its determination by atomic spectrometric techniques, namely, hydride generation atomic absorption spectrometry (HGAAS) and inductively coupled plasma mass spectrometry (ICP-MS). Chitosan was synthesized from chitin and sodium silicate was used as the immobilization matrix due to its straightforward synthesis. Through sequential sorption studies, it was shown that chitosan-immobilized sodium silicate has exhibited a better chemical stability than the chitosan itself which demonstrates the advantage of immobilization method. Both chitosan and chitosan-immobilized sodium silicate were shown to selectively adsorb As(V), arsenate, from waters at pH 3.0 at which neither chitin nor sodium silicate displayed any sorption towards As(V). The sorption of arsenate by chitosan is supposed to have electrostatic nature since pH of 3.0 is both the point at which the amino groups in chitosan are protonated and also the predominant form of As(V) is $H_2AsO_4^-$. A pre-oxidation step is required if both As(III) and As(V) are to be determined. Desorption from the sorbents was realized with 1.0% (w/v) L-cysteine prepared in a pH 3.0 solution adjusted with HCl. Among the possible interfering species tested, only Te(IV) and Sb(III) were shown to cause a decrease in the sorption capacity especially at high interferant concentrations. High concentrations of Sb(III) also resulted in gas phase interference during hydride generation.

The validity of the method was checked both via spike recovery experiments and also through the analysis of a standard reference material. Spike recovery tests were carried out with four different types of water; namely, ultra-pure, bottled drinking, tap, and sea water; and percent recovery values were found to be 114 (±4), 112 (±2), 43 (±4), and 0 (±1), respectively. It was concluded that the proposed methodology can be applied efficiently to low-to-medium ionic strength solutions, such as most drinking waters. The accuracy of the method was additionally investigated through the analysis of a standard reference material and a good correlation was found between the determined ($26.6 \pm 2.4\ \mu g\ L^{-1}$) and the certified ($26.67\ \mu g\ L^{-1}$) value.

1. Introduction

In nature, arsenic can be found in food, water and air in organic and inorganic forms [1] and exists in the −3, 0, +3 and +5 oxidation states [2–4]. Inorganic arsenic species occur as arsenite, As(III), with primary form of H_3AsO_3 and arsenate, As(V), with primary forms of $H_2AsO_4^-$ and $HAsO_4^{2-}$ in natural waters [1]. Arsenates are stable under aerobic (oxidizing) conditions whereas arsenites are predominant under anaerobic (reducing) conditions [3,5].

Both natural and anthropogenic sources contribute to the arsenic levels in the environment, which is distributed throughout earth crust, soil, water, air and living organisms [5]. The presence of arsenic in drinking water is related to the dissolution of minerals and ores [6]. Waste discharges from industrial and mining activities, agricultural use of arsenical pesticides and use of chromated copper arsenate (CCA) wood preservative may enhance the anthropogenic arsenic contamination in air, water and soil [5]. Long term consumption of drinking water contaminated with arsenic is reported to cause cancers of the skin, lungs, kidney and liver. Short term exposure to arsenic may result in vomiting, oesophageal, and abdominal pain, and "rice water" diarrhea [2,6]. Hence, drinking water containing arsenic is a potential threat to the health of humans. The World Health Organization (WHO) revised the guide-

* Corresponding author. Tel.: +90 232 7507533; fax: +90 232 7507509.
E-mail address: ahmeteroglu@iyte.edu.tr (A.E. Eroğlu).

0039-9140/$ – see front matter © 2009 Elsevier B.V. All rights reserved.
doi:10.1016/j.talanta.2009.09.053

line for arsenic in drinking water from 0.05 to 0.01 mg L^{-1} and has classified arsenic as the most toxic chemical with carcinogenic effects [6].

Because of the undesired health effects mentioned above, finding/devicing economic, easily operable and nontoxic technologies for removal of arsenic are a major goal especially when clean water sources are scarce. Arsenic removal methods from drinking water including precipitation, adsorption, ion exchange, membrane filtration and some other alternative processes have been reviewed [1,2,7]. All processes are limited with lower efficiency for arsenite removal because of the uncharged state of the species under pH 8 which necessitates the oxidation of As(III) before the removal step. In last years, nanozero valent iron has become one of the most attractive materials for arsenic removal which effectively removes both inorganic forms [8,9]. Application of various biomasses in arsenic removal has been reviewed by Mohan and Pittman [2]. Among numerous polysaccarides, cellulose and chitin are the most abundant organic compounds on the earth, with the largest amounts of production per year [10]. The shells of marine crustaceans such as crabs and shrimps are available as waste from the seafood processing industry and are used for commercial production of chitin. Chitosan, the N-deacetylated form of chitin, is an attractive material with unique properties of non-toxicity, film and fiber forming properties, adsorption of metal ions, coagulation of suspensions or solutes, and distinctive biological activities [10,11] and is produced by thermochemical alkaline treatment of chitin. Chitosan has been used as a sorbent for arsenic removal. For example, Kartal and Imamura studied arsenic removal from chromated copper arsenate (CCA)-treated wood via biosorption by chitin and chitosan in 1, 5 and 10 days periods; however, a quantitative removal was not obtained [12]. Chitosan was modified with molybdate and it was shown that the modification increased the sorption capacity by the ability of molybdate ion to complex As(V) [13–16]. Chitosan was also used as a resin for arsenic sorption in column studies with improved resistance to shrinkage which was obtained by cross-linked chitosan functionalized with 3,4-diamino benzoic acid [17]. Boddu et al. used ceramic alumina dip-coated with chitosan for As(III) and As(V) removal in column and an improved sorption capacity was reported for As(III) [18].

As revealed in the literature, effective use of chitosan as a sorbent can be based on the enhancement of its capacity through particular modifications. In the meantime, the resistance of the biomaterial to shrinkage may be improved. Immobilization of chitosan onto a supporting surface increases the surface area of sorbent (compared to chitosan itself) with a corresponding increase in the number of functional groups available for sorption. Using sodium silicate as an immobilization matrix has the advantage of tuning the immobilized amount of functional groups in a narrow synthesis time. Ease of the application and availability of low-cost chemicals are among the other advantages of the silicate-immobilization method. In this study, both chitosan as synthesized and chitosan-immobilized sodium silicate were used in the sorption of As(V) from waters prior to determination by hydride generation atomic absorption spectrometry (HGAAS) and inductively coupled plasma mass spectrometry (ICP-MS).

2. Experimental

2.1. Instrumentation and apparatus

A Thermo Elemental Solaar M6 Series atomic absorption spectrometer (Cambridge, UK) with an air-acetylene burner was used in arsenic determination utilizing the Segmented Flow Injection Hydride Generation (SFI-HGAAS) unit. An arsenic hollow cathode lamp at the wavelength of 193.7 nm and a deuterium lamp were employed as the source line and for background correction, respectively. In HGAAS, the quartz tube atomizer was 10 cm long, 8 mm in internal diameter and 10 mm in external diameter with a 4 mm bore inlet tube fused at the middle for sample introduction. Air-acetylene flame was used for heating the quartz tube externally and nitrogen was used as the carrier gas. Operating parameters for the HGAAS system were as follows: 200 mL min^{-1} carrier gas (N_2) flow rate, 6.1 mL min^{-1} HCl flow rate, 2.0% (v/v) HCl concentration, 3.0 mL min^{-1} $NaBH_4$ flow rate, 1.0% (w/v) $NaBH_4$ concentration (stabilized with 0.1%, w/v, NaOH), 7–8 mL min^{-1} sample flow rate. In addition to HGAAS, ICP-MS (Agilent 7500ce Series, Tokyo, Japan) was also employed in validation and interference studies.

In batch sorption studies, GFL 1083 water bath shaker (Burgwedel, Germany) equipped with a microprocessor thermostat was used for mixing. The elemental composition of chitosan was determined by a LECO-CHNS-932 elemental analyzer (Mönchengladbach, Germany). Determination of the molecular weight was realized using a Petrotest capillary viscosimeter (Dahlewitz, Germany). The crystallographic structure of the sorbent was elucidated by a Philips X'Pert Pro X-Ray Diffractometer (Eindhoven, The Netherlands). The pH adjustments were performed with Ino Lab Level 1 pH meter (Weilheim, Germany). Microimages of sorbents were taken utilizing a Philips XL-30S FEG scanning electron microscope (Eindhoven, The Netherlands). The thermal properties of sorbents were analyzed using a Perkin Elmer Pyris Diamond TG/DTA (Boston, MA, USA). The point of zero charge of chitosan flakes was determined with a Zeta-Meter 3.0+ equipment (Staunton, USA).

2.2. Reagents and solutions

All the chemicals were of analytical reagent grade. Ultra-pure water (18.2 MΩ) was used throughout the study. Glassware and plastic containers were cleaned by soaking in 10% (v/v) nitric acid for 24 h and rinsed with deionized water prior to use.

Stock standard solutions of As(V) and As(III), 2000.0 mg L^{-1}, were prepared by dissolving As_2O_5 (Merck, product code: 1.09939, CAS no.: [1303-28-2]) and As_2O_3 (Fischer, CAS no.: [1327-53-3]), respectively, in ultra-pure water. Stock standard solution of Te(IV), 500.0 mg L^{-1} was prepared by pre-reduction of Te(VI) (Aldrich, product code: 41058-6, CAS no.: [26006-71-3]) by boiling with 6.0 M HCl. Stock solutions of Se(VI), Se(IV), Sb(III) and Sb(V), 1000.0 mg L^{-1}, were prepared by dissolving Na_2SeO_4 (Fluka, product code: 71948, CAS no.: [13410-01-0]), $Na_2SeO_3{\cdot}5H_2O$ (Merck, product code: 1.06607, CAS no.: [26970-82-1]), $C_8H_4K_2O_{12}Sb_2{\cdot}3H_2O$ (Sigma–Aldrich, product code: P-6949, CAS no.: [28300-74-5]) and $KSb(OH)_6$ (Riedel-de Haen, product code: 31149, CAS no.: [12208-13-8]), respectively, in ultra-pure water. Mo(VI) and V(V), 1000.0 mg L^{-1} standard stock solutions were supplied from High-Purity Standards (product code: 100065-1) and Merck (product code: 1.70227), respectively. Lower concentration standard solutions were prepared daily by appropriate dilution from their stock standards before use.

Chitosan flakes were synthesized from practical grade chitin (Sigma, product code: C923, CAS no.: [1398-61-4]).

Sodium borohydride solution was prepared for a daily use from fine granular product (Merck, product code: 8.06373, CAS no.: [16940-66-2]) and stabilized by NaOH (Merck, product code: 1.06498, CAS no.: [1310-73-2]) in water. L-cysteine (Merck, product code: 1.02838, CAS no.: [52-90-4]) was added to all standards and samples to reduce As(V) to As(III) before HGAAS determination.

N,N-Dimethylacetamide (Sigma, product code: D 5511, CAS no.: [127-19-5]) containing 5.0% (w/v) LiCl (Aldrich, product code: 310468, CAS no.: [7447-41-8]) and 0.200 M NaCl (Riedel-de Haen, product code: 13423, CAS no.: [7647-14-5]) containing 0.100 M acetic acid (Riedel-de Haen, product code: 27225, CAS no.: [64-

19-7]) were used in molecular weight determination of chitin and chitosan, respectively.

$BaCl_2 \cdot 2H_2O$ (Riedel-de Haen, product code:11411, CAS no.: [10326-27-9]) was used to prepare 0.1 M solution by dissolving appropriate amount in distilled water. Silicate-immobilization matrix was prepared from sodium silicate solution (Sigma–Aldrich, product code: 338443, CAS no.: [1344-09-8]).

2.3. Synthesis and characterization of chitosan

2.3.1. Synthesis of chitosan

Chitosan flakes were synthesized from chitin under inert atmosphere by the method of Rigby and Wolfrom given in the monograph by Muzzarelli [19]. Briefly, 15.0 g of chitin was treated with 720 mL of 40.0% (w/w) aqueous NaOH solution in a 1-L three-necked round bottomed flask with reflux condenser connected to its middle neck. A thermometer was connected to control the temperature during the reaction and N_2 gas was bubbled through the solution from the side arm to provide inert atmosphere in the reaction medium. Constant reflux was obtained at 115 °C and continued for 6 h. After cooling the alkaline mixture to room temperature, chitosan flakes were washed with distilled water until a neutral filtrate was obtained. The resulting chitosan flakes were dried at 60 °C for 2 h before use.

2.3.2. Characterization of chitosan

A variety of methods were applied for the characterization of synthesized chitosan flakes. Elemental analysis and potentiometric titrimetry were used for the determination of the degree of deacetylation as reported in the literature [20,21]. The molecular weights of chitin and chitosan were determined by viscosimetric method which relates intrinsic viscosity of polymer to its molecular weight according to Mark–Houwink–Sakurada relation as described in the literature [21–26]. Images of chitosan, sodium silicate, and chitosan-immobilized sodium silicate were taken with scanning electron microscopy (SEM). XRD crystallographic properties and thermal gravimetric degradation were also investigated.

2.4. Immobilization of chitosan on sodium silicate

Chitosan was immobilized on polysilicate matrix after slight modification in the method described by Karunasagar et al. [27] in which sodium silicate was used as the immobilization matrix for the plant *Coriandrum sativum*. In the present study, the immobilization procedure was as follows: 6.0% (w/w) sodium silicate was added dropwise into 15.0 mL of 5.0% (v/v) H_2SO_4 until pH rose to 2. The solution pH was checked with pH paper instead of pH meter in order not to cause any damage to the electrode system due to use of silicate solution. Then, 50.0 mL of 2.0% (w/v) chitosan dissolved in 2.0% (v/v) acetic acid was added dropwise to the silicate solution and the mixture was stirred for 15 min. The polymer gel was formed by increasing the pH to 7 by dropwise addition of sodium silicate solution. Formed gel was washed with ultra-pure water until the solution is free of sulphate ion. This was checked by the addition of 0.200 M $BaCl_2$ solution to the filtrate. Usually cloudiness is observed as a result of precipitation reaction between barium and sulphate ions when sulphate is at an appreciable concentration. After the immobilization procedure had been completed, the chitosan-immobilized sodium silicate was dried at 50 °C overnight and ground by mortar and pestle prior to use.

2.5. Sorption studies

Sorption studies were performed for all the sorbents prepared; namely, chitin, chitosan, sodium silicate and chitosan-immobilized sodium silicate through batch process. Effect of the sorbent amount, shaking time, solution pH, reaction temperature and successive loadings was investigated. In all these experiments, batch sorption was followed by the filtration of the mixture through blue-band filter paper and analysis of the filtrate for its arsenic content using HGAAS. Before HGAAS measurements all samples and standard solutions were acidified with the addition of appropriate amount of concentrated HCl to produce 1.0% (v/v) HCl in the final solution. For As(V) determination, L-cysteine was also added to all solutions so as to have 0.5% (w/v) concentration in the final solution which guaranteed the pre-reduction of As(V) to As(III).

2.6. Sorption isotherm models

Sorption isotherm is a constant-temperature curve that describes the retention of a substance on a solid at various concentrations and is used to predict the mobility of the substance in the environment [28]. Sorption isotherm defined by Langmuir assumes that the energy of sorption is constant and sorption occurs at a fixed number of definite localized homogeneous sites with monolayer coverage [28–30]. The nonlinear form of Langmuir isotherm is given in Eq. (1):

$$Q_e = Q_{max} \frac{bC_e}{1 + bC_e} \quad (1)$$

Here, Q_{max} (mmol/g) and b (L/mmol) are Langmuir constants; Q_{max} is the amount of arsenate ion sorption corresponding to monolayer coverage, b is the affinity of arsenate for the sorbent, C_e (mmol/L) is the amount of arsenate in liquid phase at equilibrium and Q_e is the amount of arsenate adsorbed on the surface of sorbent (mmol/g) at equilibrium. The values of constants were evaluated from the linearized form of the equation which is given in Eq. (2):

$$\frac{1}{Q_e} = \frac{1}{Q_{max}} + \frac{1}{Q_{max} bC_e} \quad (2)$$

The intercept and slope of the plot of $1/Q_e$ versus $1/C_e$ were used for determination of Q_{max} and b.

Freundlich isotherm is among the most widely applied isotherms. This isotherm can be applied for heterogeneous surfaces over a wide range of concentrations. The nonlinear form of this isotherm is described by Eq. (3) [31]:

$$Q_e = K_F C_e^{1/n} \quad (3)$$

where K_F and n are constants for a given sorbent–sorbate system. These constants can be evaluated from the linearized form of Eq. (3) given as follows:

$$\log Q_e = \log K_F + \frac{1}{n} \log C_e \quad (4)$$

The intercept and slope of the plot of $\log Q_e$ versus $\log C_e$ in Eq. (4), give K_F and $1/n$, respectively.

Dubinin–Radushkevich (D–R) isotherm model assumes that the ionic species bind preferentially to most energetically favorable sites of sorbent material and allows for multilayer sorption of ions [13]. D–R isotherm is generally described by Eq. (5) [32]:

$$Q_e = q_s \exp(-B\varepsilon^2) \quad (5)$$

where

$$\varepsilon = RT \ln\left(1 + \frac{1}{C_e}\right) \quad (6)$$

The D–R parameter, B, provides information about the mean free energy of sorption defined as the energy required to transfer one mole of ions to the surface of the solid from infinity in the solution. The constant, q_s corresponds to the sorption monolayer capacity

[33]. The mean free energy of sorption can be calculated from D–R parameter B using Eq. (7):

$$E = (2B)^{-1/2} \quad (7)$$

The q_s and B constants are, respectively, obtainable from the intercept and the slope of the experimental plot of $\ln Q_e$ versus ε^2.

2.7. Desorption/dissolution studies

Two different strategies were followed to take the adsorbed arsenate ion back into solution from chitosan or chitosan-immobilized sodium silicate. Firstly, 2% (v/v) acetic acid in which chitosan was completely soluble was used. Secondly, desorption was carried out in L-cysteine which reduces the adsorbed form of arsenic (As(V), arsenate) to the non-adsorbed form (As(III), arsenite). In both strategies, calibration standards were also prepared in the same matrixes using the same method of preparation (matrix-matched standards). Before HGAAS measurements both samples and standards were acidified with concentrated HCl to produce 1.0% (v/v) of HCl in the final solution. For reduction of As(V) to As(III) L-cysteine was added to produce 0.5% (w/v) in the solution (This step was skipped if desorption matrix had already contained L-cysteine.).

2.8. Interference studies

Interference effects of two groups of compounds on arsenic determination were investigated. The first group contained hydride forming ions possessing different oxidation states of several elements; namely, Sb(III), Sb(V), Te(IV), Te(VI), Se(IV), and Se(VI) ions. The second group included Mo(VI) and V(V) for which chitosan is presumed to show sorption affinity [17,34]. Two types of interferences were expected: firstly, during the sorption of arsenate, and secondly, during hydride generation [35].

Initially, the sorption characteristics of chitosan towards each of the possible interfering ions were investigated in the absence of arsenate. For this purpose, 100.0 and 1000.0 $\mu g\,L^{-1}$ concentrations of the ions were mixed with chitosan and shaken under the conditions optimized for arsenate sorption. The percent sorption of each ion was determined by ICP-MS after acidification with concentrated HNO_3 so as to have 1.0% (w/v) acid concentration in the final solution.

In addition, 10.0, 100.0, 1000.0 $\mu g\,L^{-1}$ of each of the interfering species were added in separate experiments into both 10.0 and 100.0 $\mu g\,L^{-1}$ As(V) solutions in order to see the interference effect in presence of arsenate. The sorption experiments were performed under optimized conditions for arsenate described in the previous paragraph. After proper acidification and pre-reduction (L-cysteine) steps, ICP-MS and HGAAS were used for the analyses.

2.9. Method validation

The proposed methodology was validated both through the analysis of a standard reference material (SRM from NIST, Natural Water – Trace Elements, Cat. No. 1640) and via spike recovery experiments. Due to the absence of any information about the oxidation state of arsenic in the SRM, initial experiments were carried out in two ways: shaking with chitosan first directly, and second, after a pre-oxidation step with concentrated HNO_3. The oxidation was carried out by diluting 5.0 mL of SRM with 10.0 mL of ultra-pure water in a teflon beaker. After addition of 3.0 mL concentrated HNO_3, heating was applied on hot plate until evaporation of solution was completed. The remaining residue was dissolved in about 10 mL of ultra-pure water and after pH was adjusted to 3.0, the solution was diluted to exactly 15.0 mL to provide an As(V) concentration of 9.0 $\mu g\,L^{-1}$ in the final solution. The same procedure was also applied to the SRM directly without pre-oxidation step. In line with these experiments, both As(III) and As(V) standard solutions were also subjected to the same procedure; namely, with or without pre-oxidation with HNO_3.

Spike recovery tests were performed with four different types of water; namely, tap, distilled, sea and bottled drinking water. Spiked samples were subjected to the same sorption/elution cycles as previously and recoveries were calculated.

In addition to the validation tests described above, solutions containing both As(III) and As(V) were analyzed with the proposed method to see if there is a mutual interference. In these experiments, both chitosan and chitosan-immobilized sodium silicate were used in a two-stage batch type process. Three different solutions, namely, As(III) only, As(V) only and the mixture of As(III) and As(V) were prepared in a way that the concentrations of the species were 100.0 $\mu g\,L^{-1}$ in each case. After the addition of 50.0 mg of chitosan or chitosan-immobilized sodium silicate, the mixture was shaken for 30 min and then was filtered through blue-band filter paper. The solid and the liquid parts were separated and the filtrate was kept for determination of its arsenic concentration. Solid chitosan (or chitosan-immobilized sodium silicate) remained on the filter paper was taken into 30.0 mL of 1.0% (w/v) L-cysteine solution of which pH was adjusted to 3.0 and shaking was continued for a further 30 min for desorption. This eluate was analyzed by ICP-MS for its arsenic concentration by using matrix-matched standards which were prepared under the same sorption/desorption conditions described above.

3. Results and discussion

3.1. Characterization of chitosan

Surface morphology of chitosan flakes, sodium silicate and chitosan-immobilized sodium silicate was examined from different locations on their surfaces using SEM. The images (not shown) reveal the increasing surface porosity of chitosan-immobilized sodium silicate in comparison to chitosan.

The thermal gravimetric analysis of chitosan shows two notable weight loss stages (Fig. 1). The first stage results in about 9% loss in weight and corresponds to the weight loss of water molecules adsorbed onto surface (25–98 °C) and weight loss of bonded water (98–266 °C). The second stage weight loss occurred between 266 and 328 °C due to rapid thermal degradation of chitosan and resulted in 33% weight loss. The results are in agreement with thermal gravimetric analysis reported for chitosan by different studies in the literature [36,37]. As in the case of chitosan, sodium silicate matrix shows a weight loss of about 9% in the same temperature range due to release of water molecules from the structure. The chitosan-immobilized sodium silicate demonstrates intermediate thermal characteristics between chitosan and immobilization

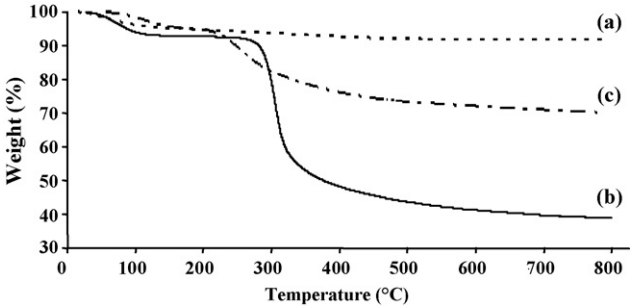

Fig. 1. TGA curves of (a) sodium silicate, (b) chitosan and (c) chitosan-immobilized sodium silicate.

matrix. Careful investigation of the weight loss percentages in thermograms is also indicative of around 30% (w/w) of chitosan in the immobilization matrix of silicate.

The degree of deacetylation of chitosan was determined by two methods: elemental analysis and titrimetry, and the results obtained were in good agreement (84.7% versus 85.4%, respectively). In addition, the percentage of chitosan-immobilized onto sodium silicate was calculated from the carbon ratios of chitosan-immobilized sodium silicate to pure chitosan sample. The amount of chitosan in sodium silicate matrix was calculated as 33.3% in the total mass which is also in accordance with TGA results.

Molecular weights of chitin and chitosan were determined using the Mark–Houwink–Sakurada equation [21–26] and found to be 1215 and 910 kDa, respectively. These results are in accordance with the results in the literature where very scattered molecular weights are reported. The wide range of the reported molecular weight values, especially for chitin, is thought to be arising from the limited solubility of chitin in the given solvent system which prevents accurate determination of the molecular weight. As reported in [26 and the references therein], two factors are effective on incomplete dissolution. Firstly, high molecular weight chitin chains are not soluble, and secondly, the presence of proteins in the unpurified chitin may associate with the N-acetyl groups in the structure and make the product insoluble. To eliminate the possible error in the determination of the molecular weight of the chitin, the insoluble part was filtered, dried, and weighed as suggested in [26]; and the true molecular weight of the chitin was calculated after subtracting the weight of the insoluble part from the total weight taken at the beginning. The calculated molecular weights indicate that the chitin used in this study is of high molecular weight and the deacetylation process not only removes the acetyl groups but also decreases the molecular weight of chitosan by cleavage of glycosidic bonds.

The X-ray diffraction patterns for chitin and chitosan are given in Fig. 2. The most significant difference observed between the two XRD patterns is the decreasing crystallinity of the compound after deacetylation process. Deacetylation procedure involves the disappearance of small peaks; only the peaks at $2\theta = 9–10^\circ$ and $2\theta = 19–20^\circ$ remain. The decrease in the crystallinity when going from chitin to chitosan was also observed by different research groups in the literature who reported that the retained peaks corresponded to hydrated crystals of chitosan [38,39].

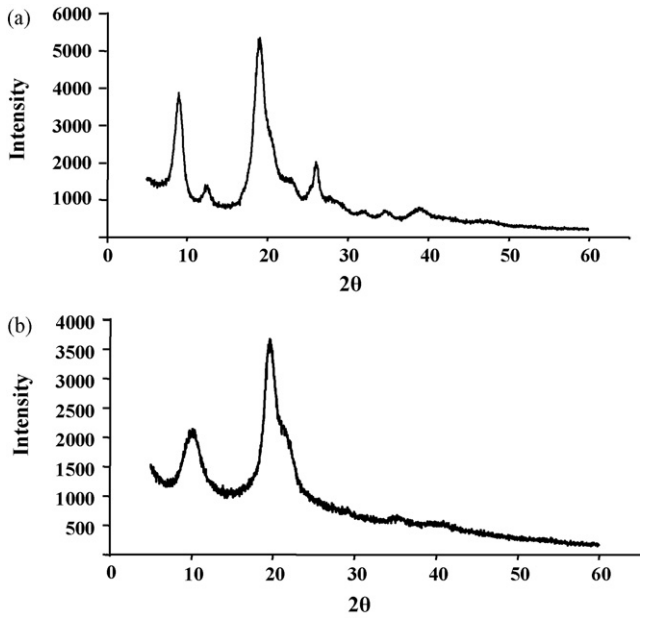

Fig. 2. X-ray diffraction patterns for (a) chitin and (b) chitosan.

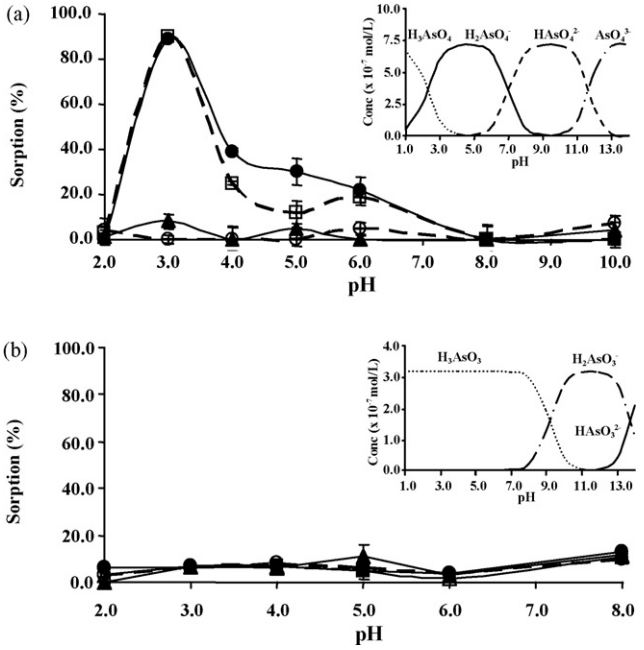

Fig. 3. Effect of pH on the sorption of (a) 100.0 μg L^{-1} As(V) and (b) 40.0 μg L^{-1} As(III) solutions. (●) chitosan, (○) sodium silicate, (▲) chitin, (□) chitosan-immobilized sodium silicate, $n = 3$. Reaction conditions: 30.0 mL sample volume, 30 min shaking time, 50.0 mg sorbent, 25 °C sorption temperature. The insets obtained with VISUAL MINTEQ software show speciation diagrams of As(V) and As(III).

3.2. Sorption studies

3.2.1. Effect of pH on sorption of As(V) and As(III)

The sorption characteristics of chitin, chitosan, sodium silicate and chitosan-immobilized sodium silicate towards As(V) and As(III) are given in Fig. 3. Chitosan and chitosan-immobilized sodium silicate have maximum sorption at pH 3.0 while sodium silicate and chitin do not show any affinity for As(V) as indicated in the figure. In case of As(III), all sorbents showed the same trend; arsenite ions were not adsorbed significantly (<15% sorption) by any of the sorbents under the working conditions applied. The nature of sorption behavior of chitosan at pH 3.0 can be explained by the electrostatic attraction between the protonated amine groups of chitosan and $H_2AsO_4^-$ ion, which is the main (approximately 85% of the As(V)) species at pH 3.0 (Fig. 3a inset). Chitosan flakes start to dissolve below pH 3 and this property precludes the possibility of them to be used as a biosorption material below this pH. Through zeta potential measurements, the isoelectric point of chitosan was determined to be 4.8–4.9. As the pH of the solution was lowered, positive charge on chitosan flakes increased. This also supported the electrostatic nature of the sorption. As can be seen from the speciation graphs of As(V) and As(III) (Fig. 3 insets), there is no any other pH with the same electrostatic behavior that biosorbent and arsenic species have opposite charges.

3.2.2. Effect of sorbent amount and shaking time on the sorption of As(V)

The percentage sorption of As(V) as a function of different amounts of chitosan and chitosan-immobilized sodium silicate is given in Fig. 4. As seen from the figure, similar sorption percentages were obtained with both sorbents at each amount tested; and 50.0 mg appeared to be the optimum amount for both sorbents under the conditions applied (the concentrations employed were

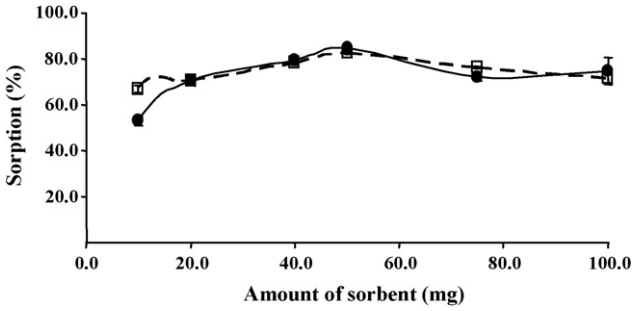

Fig. 4. Effect of sorbent amount on the sorption of 30.0 mL 100.0 μg L^{-1} As(V) solution at pH 3.0, 25 °C sorption temperature. (●) chitosan, (□) chitosan-immobilized sodium silicate, $n = 3$.

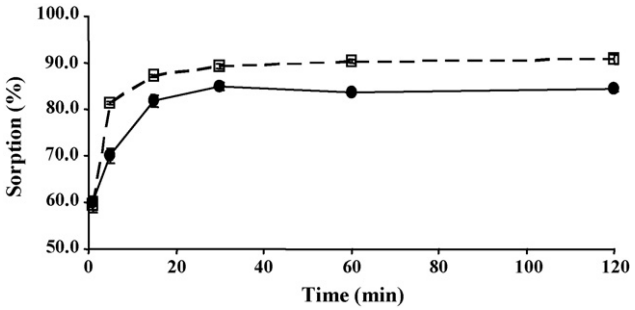

Fig. 5. Effect of shaking time for 50.0 mg sorbent at pH 3.0 in 30.0 mL 100.0 μg L^{-1} As(V) solution at 25 °C sorption temperature. (●) chitosan, (□) chitosan-immobilized sodium silicate, $n = 3$.

lower than the sorption capacity of the sorbents). Otherwise, the amount of chitosan-immobilized sodium silicate would be about three times that of the chitosan itself since the immobilized sorbent contains about 33% chitosan. This behavior can also be explained by the increased surface area of the immobilized sorbent (32.6 m^2/g) compared to that of chitosan (9.1 m^2/g).

Effect of shaking time on the percentage sorption was investigated for 1, 5, 15, 30, 60 and 120 min; the results are given in Fig. 5. As seen in the figure, the results are very similar for both sorbents especially after 15 min which can be taken as the equilibration time. However, the sorption rate before 15 min for the immobilized sorbent was sharper than that of chitosan which can be the indication of less diffusion restricted sorption in chitosan-immobilized sodium silicate.

3.2.3. Effect of solution temperature on the sorption of As(V)

The extent of sorption of As(V) by chitosan and chitosan-immobilized sodium silicate decreases as temperature increases. This behavior is reflected into the negative values of ΔH^o, given in Table 1, which designate the exothermic nature of sorption. The negative ΔS^o values suggest that sorption is associated with a decrease in system entropy probably due to the restriction on the mobility of the sorbate ions that results from binding to the sorbent surface. The process thus appears to be enthalpy-driven. Both parameters contribute to negative ΔG^o values which in turn results when the equilibrium position of a reaction occurs closer to the products.

Table 1
Thermodynamic parameters of chitosan and chitosan-immobilized sodium silicate (50.0 mg sorbent, 30.0 mL of 100.0 μg L^{-1} As(V) at pH 3.0, $n = 3$).

	ΔG^o (kJ/mol)		ΔH^o (kJ/mol)	ΔS^o (J/mol K)	
	298 K	323 K		298 K	323 K
Chitosan	−20.2	−19.8	−24.7	−15.1	−15.1
Chitosan-immobilized sodium silicate	−21.1	−20.9	−23.8	−9.1	−9.1

3.2.4. Successive loading

Sequential sorption of arsenate by chitosan and chitosan-immobilized sodium silicate for two different concentrations was investigated. It can be seen from Fig. 6a that the sorption percentage starts to decrease with the third loading and previously sorbed arsenate even starts to be released from chitosan surface after the sixth loading. This observation cannot be related to the sorption capacity of chitosan since a similar trend was observed for both 100.0 and 1000.0 μg L^{-1} concentrations. In order to clarify this further, the cumulative amount of arsenate on the sorbent was also determined which was approximately 0.015 mmol/g at the sixth load. This amount is still lower than the maximum sorption capacity of chitosan. Several reasons can be suggested to explain the decrease in sorption capacity. Firstly, a gradual dissolution of flakes was observed after each loading which might have caused a decrease in the sorption capacity. More importantly, the dissolution of chitosan flakes must have been associated with the release of previously adsorbed species from the surface which eventually increased the arsenate concentration in the solution. Secondly, although it needs further consideration, it can be speculated that the surface positive charge of chitosan after each loading could have been reduced which might also have resulted in a decrease in the sorption percentage after each step.

In contrast to chitosan, chitosan-immobilized sodium silicate has shown a better chemical stability in a way that no negative sorption (no release from chitosan surface) was observed although the sorption percentage started to decrease after the second load for both concentrations (Fig. 6b). As in the case of chitosan, the decrease in the sorption percentage of chitosan-immobilized sodium silicate cannot be explained by the reduction in the sorption capacity of the immobilized sorbent. Similarly, from the cumulative amount of arsenate on the immobilized sorbent, the amount of arsenate even at the tenth load is approximately 0.016 mmol/g which is about half of the maximum sorption capacity of chitosan-immobilized sodium silicate.

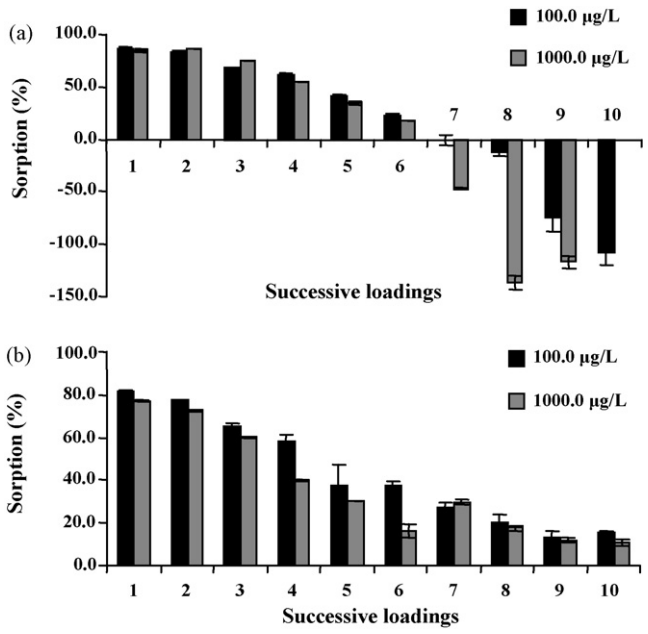

Fig. 6. Percent sorption of (a) chitosan and (b) chitosan-immobilized sodium silicate for 10 successive loadings in pH 3.0, 30.0 mL of 100.0 and 1000.0 μg L^{-1} As(V) concentrations, 50.0 mg sorbent, 30 min at 25 °C batch sorption, $n = 3$.

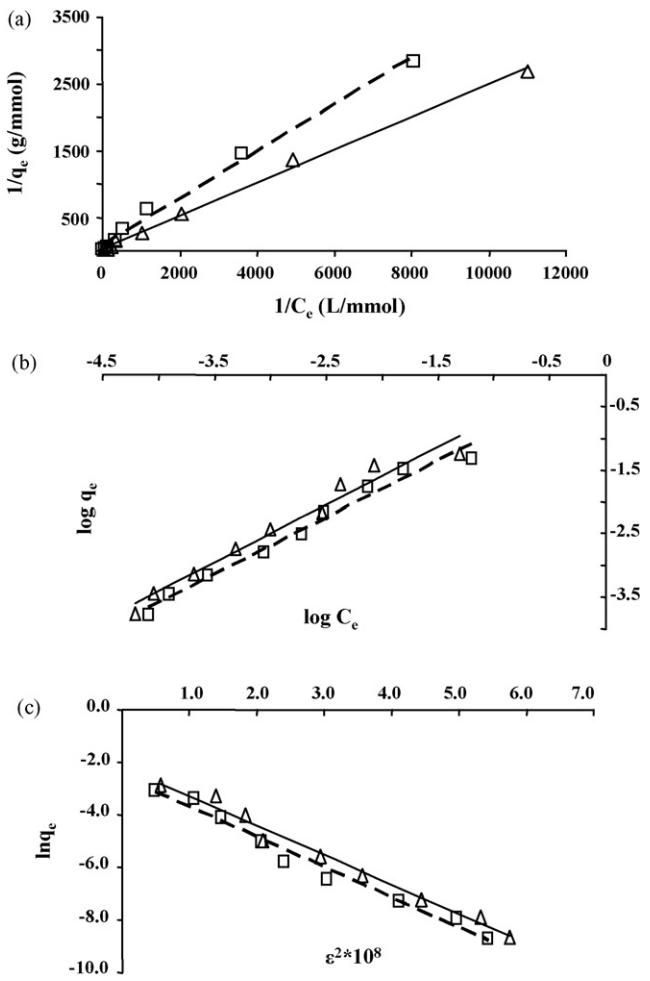

Fig. 7. Linear fits of (a) Langmuir, (b) Freundlich, (c) Dubinin–Radushkevich models for arsenate sorption by (△) chitosan and (□) chitosan-immobilized sodium silicate.

3.3. Sorption isotherm models

Freundlich, Dubinin–Radushkevich and Langmuir isotherm models were tested for sorption of arsenate by chitosan and chitosan-immobilized sodium silicate. The linearized forms of models (Fig. 7) were used for the calculation of coefficients and the results are summarized in Table 2. According to the linear correlation coefficients (R^2), Langmuir model, with R^2 close to unity, appears as the most suitable isotherm for describing the sorption of arsenate on chitosan and chitosan-immobilized sodium silicate. However, D–R isotherm can be considered also to provide adequate description of the sorption data.

3.4. Desorption studies

As described in Section 2.7, two different elution strategies were followed to take the sorbed arsenate ion back into solution from chitosan or chitosan-immobilized sodium silicate. In the first method, 2% (v/v) acetic acid was used and chitosan was completely dissolved together with the previously sorbed arsenate. On the other hand, in the case of chitosan-immobilized sodium silicate, acetic acid was not effective even though acid concentration and volume, and desorption time were doubled. Therefore, as a second method, 1.0% (w/v) L-cysteine prepared in a pH 3.0 solution adjusted with HCl was used as the eluent which was expected to reduce the adsorbed arsenate (As(V)) to arsenite (As(III), non-adsorbed form) through the thiol groups [35 and the references therein]. In the meantime, arsenic in the solution was converted to the hydride forming form. This eluent worked with 100% efficiency and was used in all desorption studies.

3.5. Interference studies

As explained in Section 2.8, two groups of possible interferants were prepared; the first group contained the hydride forming elements; namely, Sb(III), Sb(V), Te(IV), Te(VI), Se(IV), and Se(VI) ions, and the second group included the oxyions of Mo(VI) and V(V) which are expected to be adsorbed by chitosan. It should also be mentioned that the interference effect was classified into two: firstly, whether the ion caused the sorption to increase-or-decrease at least 30% of the original signal obtained with As(V) only, and secondly, the adsorbed ion caused at least 30% increase-or-decrease in the hydride signal of As. For this purpose, all the solutions were analyzed with both HGAAS and ICP-MS.

As a starting point, the sorption of chitosan towards each of the ions mentioned above was investigated under the conditions optimized for arsenate sorption but in the absence of arsenate; and it was found that chitosan shows affinity to all species except Te. The sorption percentage was almost 100% for Mo(VI), V(V) and Se(VI) in both concentrations; namely, 100.0 and 1000.0 $\mu g\,L^{-1}$. These results were in agreement with several studies of Guibal et al. in which they report that the sorption of Mo(VI) by cross-linked chitosan beads was maximum at pH 3 [13]. Similarly Qian et al. found that optimum pH value for maximum sorption of V(V) ions was 3 [40].

No interference was observed from neither Se(IV) nor Se(VI) for an As(V) concentration of 10.0 $\mu g\,L^{-1}$ although chitosan shows high affinity for Se(VI). On the other hand, when As(V) concentration was 100.0 $\mu g\,L^{-1}$, a decrease in sorption percentage was observed in the presence of 1000.0 $\mu g\,L^{-1}$ Se(IV). Sb(V) and Sb(III)

Table 2
Summary of models coefficients (Solution volume, shaking time, solution pH, sorbent amount and reaction temperature were 30.0 mL, 30 min, pH 3.0, 50.0 mg, and 25 °C, respectively, $n = 3$.).

Adsorption model	Parameter	Chitosan	Chitosan-immobilized sodium silicate
Langmuir	R^2	0.9963	0.9918
	Q_{max} (mmol/g)	0.03038	0.01276
	B (L/mmol)	133.43	222.25
Freundlich	R^2	0.9649	0.9781
	K_F	1.655	0.9309
	$1/n$	0.9054	0.8883
Dubinin–Radushkevich	R^2	0.9822	0.9804
	B (mol/kJ)^2	1×10^{-8}	1×10^{-8}
	q_s	0.1166	0.0781
	E (kJ/mol)	7.07	7.07

Table 3
The comparative spike recovery of As(V) and As(III) ions from chitosan and chitosan-immobilized sodium silicate (Sorption conditions: solution volume, shaking time, solution pH, sorbent amount and reaction temperature were 30.0 mL, 30 min, pH 3.0, 50.0 mg, and 25 °C, respectively, $n = 3$; elution conditions: eluent volume, shaking time, solution pH and reaction temperature were 30.0 mL of 1.0% (w/v) L-cysteine solution, 30 min, pH 3.0 and 25 °C, respectively, $n = 3$.).

Solution	Spike recovery (%)			
	Chitosan		Chitosan-immobilized sodium silicate	
	ICP-MS	HGAAS	ICP-MS	HGAAS
100.0 μg L^{-1} As(V)	110.0 (±3.7)	96.3 (±2.5)	104.6 (±3.5)	102.2 (±5.8)
100.0 μg L^{-1} As(III)	10.6 (±0.4)	10.0 (±0.7)	13.1 (±0.2)	13.6 (±2.3)
100.0 μg L^{-1} As(V) + 100.0 μg L^{-1} As(III)	111.2 (±2.4)	95.9 (±3.3)	104.1 (±1.0)	102.4 (±2.7)

behaved differently from the other hydride forming elements in a way that they caused a decrease in hydride signal of arsenic when their concentrations were 1000.0 μg L^{-1}. This finding is in accordance with the results obtained in one of our earlier studies which was about the gas phase interference of Sb(III) during hydride formation in HGAAS system [41]. The interference caused only during hydride formation can be eliminated with the use of ICP-MS if it is available in the laboratory. An unexpected interference (decrease in the arsenate sorption percentage by chitosan) was observed for both As(V) concentrations in the presence of 1000.0 μg L^{-1} Te(IV). As mentioned in the previous paragraph, chitosan demonstrates a very low affinity to Te(IV) (<1%) under the optimized sorption conditions for As(V). It should not be speculated much on this observation; but it can be stated that the presence of Te(IV) may change the reaction conditions during the sorption of As(V) by chitosan which needs further investigation. Although chitosan showed high affinity for V(V), this property did not cause any reduction in the signal due to the high capacity of chitosan. Instead, V(V) caused a small increase in As(V) sorption which necessitates the close control of this oxyion in the sample matrixes. Totally different behavior was obtained in the case of Mo(VI) for two different As(V) concentrations; when As(V) was only 10.0 μg L^{-1}, none of the Mo(VI) concentrations caused interference. However, when As(V) and Mo(VI) concentrations were both 100.0 μg L^{-1}, a decrease in the sorption capacity of chitosan towards As(V) was observed.

3.6. Method validation

The proposed methodology was validated, as explained in Section 2.9, both via spike recovery experiments and also through the analysis of a standard reference material. Initially, arsenate/arsenite speciation was performed using chitosan and chitosan-immobilized sodium silicate. As seen in Table 3, both chitosan and chitosan-immobilized sodium silicate have been found effective in arsenate recovery from spiked solutions whereas they have demonstrated a very low sorption (about 10%) towards arsenite. In addition to the above solutions containing only one arsenic species, either As(V) or As(III), solutions containing both As(III) and As(V) were analyzed with the proposed method to see if the presence of As(III) affected the sorption of As(V). The results indicate that sorption of As(V) is not affected from the presence of As(III) under the conditions employed as expected and this demonstrates the arsenic speciation capability of the chitosan and the chitosan-immobilized sodium silicate.

Subsequently, spike recovery tests were also carried out with four different types of water; namely, ultra-pure, bottled drinking, tap, and sea water. Spiked samples were subjected to the same sorption/elution cycles as previously. The results given in Table 4 show that the proposed methodology works efficiently for ultra-pure and bottled drinking water samples where the recovery values were very close to 100%. The municipality tap water of Urla where the IYTE campus is situated is very hard with high carbonate content. The hard matrix of this tap water had caused a change in Sb(III)/Sb(V) equilibrium in a previous study in which the use of L-cysteine was required to reduce Sb(V) to Sb(III) before the sorption of Sb(III) by Duolite GT-73 chelating resin [42]. Here, the low recovery value given in Table 4 (43.2%) is thought to be due to the high ionic strength of the tap water rather than its effect on the As(III)/As(V) equilibrium. The situation was even worst in the case of spiked sea water in which arsenate could not be recovered because of the very high ionic strength of the solution.

Finally, the accuracy of the proposed methodology was investigated through the analysis of a standard reference material, SRM from NIST (Natural Water – Trace Elements, Cat. No. 1640). Since the oxidation state of arsenic was not stated in the certificate, the SRM was analyzed both with and without a pre-oxidation step and the results compared. The same strategy was also followed with both As(III) and As(V) standard solutions to see the effect of the pre-oxidation step. As expected, SRM and As(III) solutions gave almost the same recovery value of 0% which also showed the importance of pre-oxidation step for unknown samples. When HNO_3 pre-oxidation step was applied, As(V) signal was assumed to be the reference (matrix-matched standard) and As(III) signal was compared to this signal after being oxidized to As(V). A conversion of 95% indicated the success of the oxidation process which also guaranteed the As(III) → As(V) conversion in the SRM. The results demonstrate the good agreement between the result of the proposed method (26.6 ± 2.4 μg L^{-1}) and the certified value (26.67 μg L^{-1}). This strong agreement may also indicate the validity of the method to the natural water samples of low and intermediate ionic strength.

Table 4
Percent recovery for spiked arsenate ion with ultra-pure, bottled, tap and sea water samples after desorption from chitosan (Sorption parameters: solution volume, shaking time, solution pH, sorbent amount and reaction temperature were 15.0 mL, 30 min, pH 3.0, 50.0 mg, and 25 °C, respectively, $n = 3$.).

Water type	Spiked As(V) concentration (μg L^{-1})		
	Initial	Final	Recovery %
Ultra-pure	10.0	11.4 (±0.5)	114.2 (±4.5)
Bottled drinking	10.0	11.2 (±0.2)	112.3 (±1.6)
Tap	10.0	4.3 (±0.4)	43.2 (±4.2)
Sea	10.0	0.0 (±0.1)	0.0 (±0.8)

4. Conclusions

It has been shown that chitosan and chitosan-immobilized sodium silicate can be applied in the sorption of As(V) from several water types. Sodium silicate as an immobilization matrix has the advantage of tuning the immobilized amount of biomass, in this case chitosan, in a narrow synthesis time. The optimum pH for As(V) sorption for both the chitosan and chitosan-immobilized sodium silicate was shown to be 3.0 at which amino groups of chitosan are protonated and the predominant form of As(V) is $H_2AsO_4^-$. Therefore, sorption was assumed to be electrostatic in nature. Speciation of As species was shown to be feasible since no sorption was obtained for As(III) at any pH investigated. If both As(III) and As(V) are to be determined, a pre-oxidation step is necessary. Desorption from the sorbents was realized with 1.0% (w/v) L-cysteine prepared in a pH 3.0 solution adjusted with HCl.

Among the isotherm models tested, Langmuir model appeared to be the most appropriate. Sorption of As(V) by the two sorbents decreased with increase in solution temperature. This exothermic behavior is associated with a decrease in system entropy. Through sequential sorption studies, it was shown that chitosan-immobilized sodium silicate has exhibited a better chemical stability than the chitosan itself which demonstrates the advantage of immobilization strategy.

The results of the interference study have shown that As(V) sorption by chitosan can be decreased especially at high interferant concentration. An exception to this observation was obtained with Sb species which caused gas phase interference during hydride generation rather than decreasing the sorption percentage. In addition, when the concentration of As(V) is 100.0 $\mu g\,L^{-1}$, the presence of V(V) in the samples causes an increase in As(V) sorption.

It can be concluded that the chitosan and chitosan-immobilized sodium silicate sorbents can be used in the sorption/speciation of As(V) from medium-to-low ionic strength solutions prior to its determination with atomic spectrometric techniques like AAS, ICP-AES, or ICP-MS. In addition, the sorbents can be used in the removal of As(V) (or As(III) after a proper oxidation step) from drinking water.

Acknowledgements

The authors would like to thank the Center of Material Research and the Environmental Research Center at İzmir Institute of Technology for the facilities SEM, TGA, XRD, and ICP-MS measurements, respectively.

References

[1] United States Environmental Protection Agency, UESPA, 1999. Doc. EPA 815-P-01-001.
[2] D. Mohan, C.U. Pittmant, J. Hazard. Mater. 142 (2007) 1.
[3] P.L. Smedley, D.G. Kinniburgh, Appl. Geochem. 17 (2001) 517.
[4] L. Ebdon, L. Pitts, R. Cornelis, H. Crews, O.F.X. Donard, P. Quevauviller, Trace Element Speciation for Environment, Food and Health, The Royal Society of Chemistry, Cambridge, 2001.
[5] B.K. Mandaland, K.T. Suzuki, Talanta 58 (2002) 201.
[6] World Health Organization, Guidelines for Drinking-water Quality [electronic resource]: Incorporating First Addendum, vol.1, Recommendations, 3rd ed., 2006.
[7] T.S.Y. Choong, T.G. Chuah, Y. Robiah, F.L.G. Koay, I. Azni, Desalination 217 (2007) 139.
[8] V.T. Nguyen, S. Vigneswaran, H.H. Ngo, H.K. Shon, J. Kandasamy, Desalination 236 (2009) 363.
[9] M.E. Morgada, I.K. Levy, V. Salomone, S.S. Farıas, G. Lopez, M.I. Litter, Catal. Today (2008), doi:10.1016/j.cattod.2008.09.038.
[10] K. Kurita, Mar. Biotechnol. 8 (2006) 203.
[11] M.N.V. Kumar, React. Funct. Polym. 46 (2000) 1.
[12] S.N. Kartal, Y. Imamura, Bioresour. Technol. 96 (2005) 389.
[13] E. Guibal, S. Milot, J.M. Tobin, Ind. Eng. Chem. Res. 37 (1998) 1453.
[14] L. Dambies, T. Vincent, A. Domard, E. Guibal, Biomacromolecules 2 (2001) 1198.
[15] L. Dambies, T. Vincent, E. Guibal, Water Res. 36 (2002) 3699.
[16] P. Chassary, T. Vincent, E. Guibal, React. Funct. Polym. 60 (2004) 137.
[17] A. Sabarudin, K. Oshita, M. Oshima, S. Motomizu, Anal. Chim. Acta 542 (2005) 207.
[18] V.M. Boddu, K. Abburi, J.L. Talbott, E.D. Smith, R. Haasch, Water Res. 42 (3) (2007) 633.
[19] R.A.A. Muzzarelli, Natural Chelating Polymers, Pergamon Press, Hungary, 1973.
[20] A. Tolaimate, J. Desbrieres, M. Rhazi, A. Alagui, M. Vincendon, P. Vottero, Polymer 41 (2000) 2463.
[21] M.R. Kasaai, J. Arul, G. Charlet, J. Polym. Sci. Polym. Phys. 38 (2000) 2591.
[22] M.R. Kasaai, Carbohydr. Polym. 68 (2007) 477.
[23] M.L. Tsaih, R.H. Chen, J. Appl. Polym. Sci. 71 (1999) 1905.
[24] S.M. Taghizadeh, G. Davari, Carbohydr. Polym. 64 (2006) 9.
[25] R.F. Weska, J.M. Moura, L.M. Batista, J. Rizzi, L.A.A. Pinto, J. Food Eng. 80 (2007) 749.
[26] M. Poirier, G. Charlet, Carbohydr. Polym. 50 (2002) 363.
[27] D. Karunasagar, M.V.B. Krishna, S.V. Rao, J. Arunachalam, J. Hazard. Mater. 18 (2005) 133.
[28] G. Limousin, J.P. Gaudet, L. Charlet, S. Szenknect, V. Barthes, M. Krimissa, Appl. Geochem. 22 (2007) 249.
[29] L. Qi, Z. Xu, Colloid Surf. A 251 (2004) 183.
[30] S. Gueu, B. Yao, K. Adouby, G. Ado, Int. J. Environ. Sci. Technol. 4 (2007) 11.
[31] R.J. Umplebay II, S.C. Baxter, M. Bode, J.K. Berch Jr., R.N. Shaha, K.D. Shimizu, Anal. Chim. Acta 435 (2001) 35.
[32] D. Kavitha, C. Namasivayam, Dyes Pigments 74 (2007) 237.
[33] A. Şeker, T. Shahwan, A.E. Eroğlu, S. Yılmaz, Z. Demirel, M.C. Dalay, J. Hazard. Mater. 154 (2008) 973.
[34] E. Guibal, Sep. Purif. Technol. 38 (2004) 43.
[35] J. Dedina, D.L. Tsalev, Hydride Generation Atomic Absorption Spectrometry, Willey, Chichester, 1995.
[36] G. Huacai, P. Wan, L. Dengke, Carbohydr. Polym. 66 (2006) 372.
[37] F.A.A. Tirkistani, Polym. Degrad. Stabil. 60 (1998) 67.
[38] M. Jaworska, K. Sakurai, P. Gaudon, E. Guibal, Polym. Int. 52 (2003) 198.
[39] K. Ogawa, Agric. Biol. Chem. 55 (1991) 2375.
[40] S. Qian, H. Wang, G. Huang, S. Mo, W. Wei, J. Appl. Polym. Sci. 92 (2004) 1584.
[41] M. Yersel, A. Erdem, A.E. Eroğlu, T. Shahwan, Anal. Chim. Acta 534 (2005) 293.
[42] A. Erdem, A.E. Eroğlu, Talanta 68 (2005) 86.